

Creep resistance and high temperature strength of poly(*p*-xylylene) fibers

H. van der Werff and A. J. Pennings*

Department of Polymer Chemistry, University of Groningen, Nijenborgh 16,
NL-9747 AG Groningen, The Netherlands

Summary

High-strength and high-modulus poly(*p*-xylylene) (PPX) fibers show no creep at room temperature and retain at 200 °C, in air or in nitrogen atmosphere, still 50 to 60 % of their tensile strengths at room temperature, whereas the modulus does not change. In stress relaxation experiments PPX fibers have relaxed after 17.4 hours less than 4 % of the initial stress whereas during the same period of time polyethylene fibers relax over 75 % of the initial stress.

Introduction

High-strength and high-modulus PPX fibers can be readily prepared by hot-drawing of the high molecular weight as-polymerized material [1]. Tensile strengths of 3.0 GPa and moduli of 100 GPa can be achieved. Up to now, interest in PPX has been mainly aroused by its unique polymerization process [2,3] and its high resistance towards electron beam irradiation [4]. This last property permitted the material to be studied by high-resolution electron microscopy, in single crystals [5–7] or in hot-drawn fibers [8].

The aim of the work presented in this paper is to explore properties of PPX fibers with respect to creep and high-temperature strength. These properties can be of crucial importance for technological applications of polymeric fibers. High-strength and high-modulus fibers of ultra-high molecular weight polyethylene (UHMWPE) can be prepared by gel-spinning and consequent hot-drawing [9]. Although a tensile strength of 7.2 GPa [10] and a Young's modulus of 264 GPa [11] can be achieved at room temperature, these fibers have some disadvantages: tensile strength decreases significantly for increasing temperature and is zero at temperatures above 152 °C [12]. Furthermore, UHMWPE fibers are very susceptible to creep [13]. Poly(*p*-phenylene terephthalamide) fibers show essentially no creep and excellent high-temperature strength, but have to be spun from solutions in concentrated sulphuric acid [14]. It is therefore of technological interest to examine additional fiber properties, apart from tensile strength and modulus, and compare these to properties of other fibers in order to estimate the full potential of high-strength and high-modulus PPX fibers.

Experimental

High-strength PPX fibers were prepared by drawing of the as-polymerized material at 420 °C, as described previously [1]. As-polymerized PPX was kindly supplied to us by Union Carbide Co.. Gel-spun UHMWPE fibers were prepared by standard procedures

*To whom offprint requests should be sent

in our laboratory [9] from linear polyethylene Hifax 1900 ($M_w = 5.5 \times 10^6$, $M_n/M_w = 3$). Cross-sectional areas of filaments were determined from fiber weight and length. Tensile tests and stress relaxation experiments were performed using an Instron 4301 tensile tester, equipped with a temperature cabinet, at a gauge length of 32.5 mm. For the dead load experiments, a piece of fiber was clamped at both ends. One of the clamps was fixed in position, whereas the other was freely suspended and had various weights attached. The movement of the latter was recorded by means of a linear displacement transducer coupled to a x-t recorder. Scanning electron microscopy (SEM) micrographs were taken using an ISI-DS 130 microscope operating at 40 kV, from gold-covered samples

Results and discussion

As-polymerized PPX at room temperature exhibits plastic deformation upon tensile testing. The stress-strain curve in fig.1 indicates ductile behavior and can be divided into three stages: elastic deformation (< 1.5 % strain), followed by plastic deformation (1.5-4.0 % strain) and finally crack formation leading to tensile failure (> 4.0 %). The successive transitions between these stages have been indicated by A and B in fig. 1.

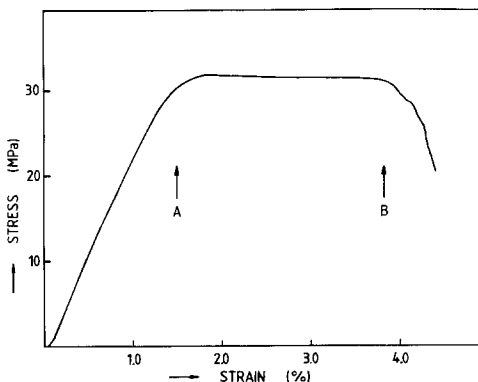


Figure 1.
Stress versus strain of as-polymerized PPX. Crosshead speed : 3.25 mm/min.

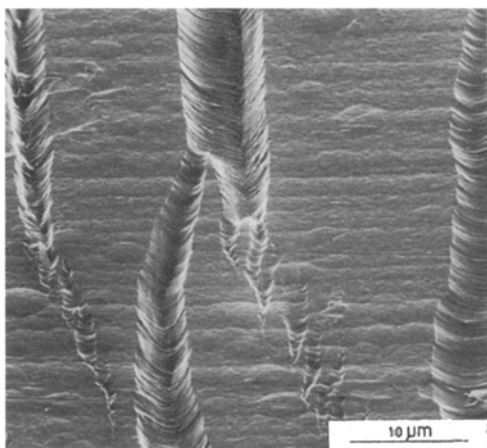


Figure 2.
SEM-micrograph of as-polymerized PPX after tensile deformation showing plastic zones in different stages of development.

SEM-micrographs clearly identify the three stages. Fig. 2 shows the existence of localized surface plastic zones, initiated at surface defects, and cracks formed inside these plastic deformation zones. Fig. 3 clearly reveals the existence of fibrils inside the plastic deformation zones prior to crack growth, and appear to be formed without noticeable formation of voids. Probably, fibrils are easily formed due to the low entanglement density in the as-polymerized material. The fracture surface is shown in fig. 4 and displays the extensive fibrillation and creation of voids due to crack growth [15]. The results from fig. 1 to 4 indicate that, at room temperature, unoriented PPX responds by flow of the polymeric chains upon tensile deformation.

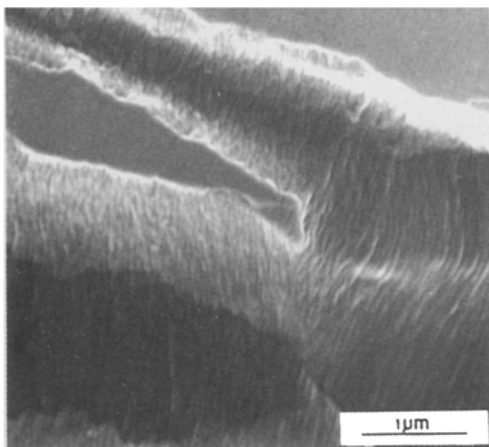


Figure 3.
SEM-micrograph of as-polymerized PPX after tensile deformation. Fibrils of about 50 nm in diameter appear to be directly formed without noticeable voiding.

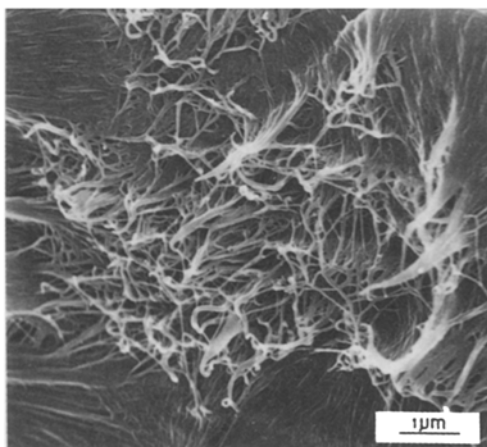


Figure 4.
SEM-micrograph of fracture surface of as-polymerized PPX after tensile deformation, showing the formation of fibrils and voids by crack growth.

Tensile deformation at temperature close to the melting point ($T_m = 427\text{ }^{\circ}\text{C}$ [16]) of PPX results into extensive flow and the material can be drawn up to draw-ratio λ of 43 [1]. Hot-drawn PPX fibers then have a high tensile strength σ_b and modulus, and break brittle at room temperature. Fig. 5 is a plot of strain versus time during a dead-load test of a PPX fiber ($\lambda=30$, $\sigma_b = 2.3\text{ GPa}$) and a UHMWPE fiber ($\lambda=30$, 1.5 wt. %

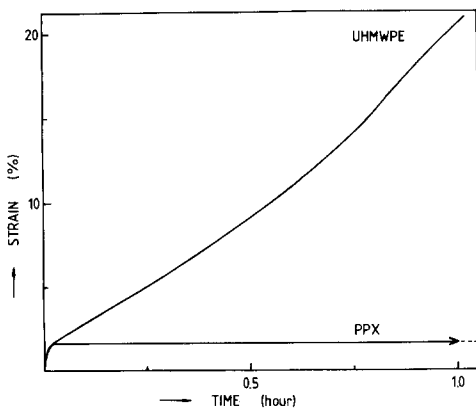


Figure 5.

Strain versus time of PPX and UHMWPE fibers during a dead-load test. Both fibers, having a tensile strength of 2.3 GPa, had loads attached corresponding to 60 % of the load at break.

gel, $\sigma_b = 2.3$ GPa). The load applied corresponds in both cases to 60 % of the load at break. The plot shows the extensive creep strain (up to 20 %) and the short time to break (1 hour) of the UHMWPE fiber. The PPX fiber, having comparable tensile properties, responds dramatically different to the application of the load. An elastic strain of about 1.6 % results, but there is no tendency to increase its length in time. Even after 306 hours, no creep strain could be measured within the accuracy of the experimental set-up (0.1 % strain) and the experiment was stopped before fiber failure occurred. The high resistance to flow of chains in oriented PPX fibers is also demonstrated by stress relaxation. In fig. 6, the stress, as a percentage of the stress at which the crosshead was stopped, is plotted as a function of time, after the fibers had been elongated to result in a tensile stress corresponding to 60 % of the tensile strength. The UHMWPE fiber ($\lambda=30$, 1.5 wt. % gel, $\sigma_b = 2.3$ GPa) again displays the ease of flow in these fibers, for it can relax over 75 % of its initial stress during 17.4 hours, whereas the PPX fiber ($\lambda=29$, $\sigma_b = 2.1$ GPa) is only able to relax about 3.6 % of its initial stress during the same period of time.

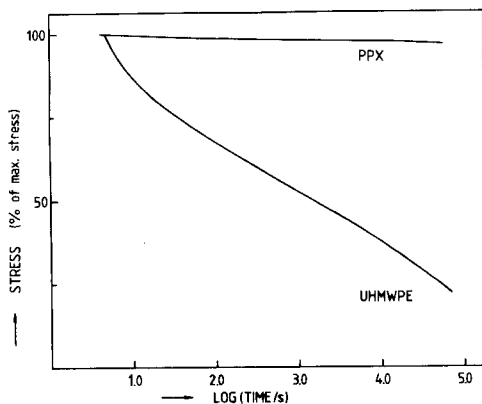


Figure 6.

Stress versus log(time) during stress relaxation of PPX and UHMWPE fibers. Both fibers were stressed up to 60 % of their tensile strengths (2.1 and 2.3 GPa, respectively). Crosshead speed : 10 mm/min. Zero time corresponds to the start of the crosshead movement.

UHMWPE fibers have zero tensile strength above 152 °C, the temperature at which the orthorhombic crystals transform into the hexagonal phase [12]. In this phase, chains can slip past each other, and the fibers will directly melt. Table 1 lists some tensile

Table 1

Tensile strength σ_b and Young's modulus E of PPX fibers at different temperatures.

Draw ratio	T = 20 °C	T = 200 °C	Atmosphere
31	$\sigma_b = 2.3$ GPa E = 90 GPa	$\sigma_b = 1.4$ GPa E = 90 GPa	nitrogen
35	$\sigma_b = 2.5$ GPa E = 93 GPa	$\sigma_b = 1.2$ GPa E = 99 GPa	air

strengths and moduli of PPX fibers tested at a temperature of 200 °C. Fibers have been tested as well in nitrogen atmosphere as in air. Tensile testing normally took place several minutes after the introduction of the fibers into the preheated temperature cabinet. The data in table 1 show that under these conditions PPX fibers still retain about 50-60 % of their original tensile strength at room temperature. The modulus is not affected by the elevated temperature. A stress-strain curve recorded at 200 °C in nitrogen atmosphere is shown in fig. 7. The stress-strain curve still shows no yielding behavior. The strain at break of 1.6 % is much smaller than the strain at break of about 3 % normally found at room temperature. Probably flaws in the fibers become increasingly fatal at higher temperatures, causing fracture at lower strains.

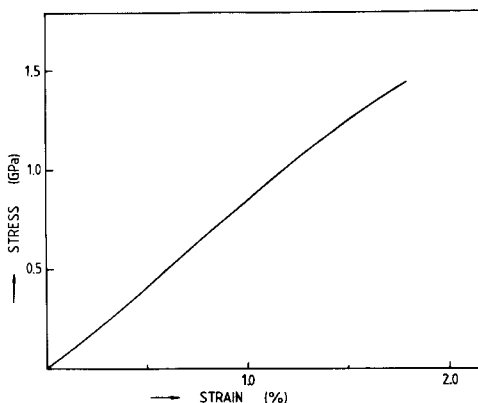


Figure 7.

Stress versus strain of a PPX fiber at 200 °C in nitrogen atmosphere. The corresponding strength at room temperature is 2.3 GPa. Crosshead speed : 10 mm/min.

The results presented here show that the as-polymerized material responds at room temperature in a ductile manner to tensile deformation. Oriented PPX fibers, however, are much less susceptible to flow, and are by far superior to UHMWPE fibers with respect to creep, stress relaxation and high-temperature strength. The high melting point of 427 °C of PPX [16] indicates the difficulty of a chain at room temperature to slip out of its crystal lattice, despite the absence of dipolar interactions and hydrogen bonding between neighbouring chains.

Combined with the fact that PPX fibers can be easily prepared in one step from as-polymerized films and no additional dissolution in a solvent is required to obtain a drawable precursor material, these results demonstrate the vast potential of PPX as a strong polymeric material.

Acknowledgements

The authors are greatly indebted to Union Carbide Co. for the provision of the as-polymerized PPX films. Furthermore, the authors would like to acknowledge J.P. Penning for his investigations on the preparation of PPX fibers and H. Nijland for taking the SEM-micrographs.

This study was supported by the Netherlands Foundation of Chemical Research (SON) with financial aid from the Netherlands Organization for the Advancement of Pure Research (NWO) and AKZO, The Netherlands.

References

1. van der Werff H, Pennings AJ (1988) *Polym Bull* 19: 587
2. Szwarc M (1947) *Discuss Faraday Soc* 2: 48
3. Gorham WF (1966) *J Polym Sci Part A-1* 3027
4. Isoda S, Ichida T, Kawaguchi A, Katayama K (1983) *Bull Inst Chem Res Kyoto Univ* 61: 222
5. Bassett GA, Keller AA (1969) *Kolloid-Z* 231: 386
6. Tsuji M, Isoda S, Ohara M, Kawaguchi A, Katayama K (1982) *Polymer* 23: 1568
7. Isoda A, Tsuji M, Ohara M, Kawaguchi A, Katayama K (1983) *Polymer* 24: 1155; idem (1983) *Makromol Chem Rapid Comm* 4: 141
8. van der Werff H, Pennings AJ, Oostergetel GT, van Bruggen EFJ (1989) *J Mat Sci Lett* 8: 231
9. Smook J, Flintermann M, Pennings AJ (1980) *Polym Bull* 2: 775
10. Pennings AJ, Roukema M, van der Veen A (1990) *Polym Bull* 23: 353
11. van der Werff H, Pennings AJ to be published
12. Dijkstra DJ, Torfs JCM, Pennings AJ (1989) *Colloid Polym Sci* 266: 866
13. Ward IM, Wilding MA (1984) *J Polym Sci Polym Phys Ed* 22: 561
14. Northolt MG, Sikkema DJ, *Lytropic Main Chain Liquid Crystal Polymers*. In: Collyer AA (ed.) *Liquid Crystal Polymers*, Elseviers Applied Science, to be published
15. Kramer EJ (1983) *Microscopic and Molecular Fundamentals of Crazing*. In: Kausch H-H (ed.) *Crazing in Polymers*, Springer, Berlin Heidelberg New York (Advances in Polymer Science, vol. 52/53, pp. 1-56)
16. Kirkpatrick DE, Wunderlich B (1985) *Makromol Chem* 186: 2595